EXPLOSIVE EMISSION AND GAP CLOSURE FROM A RELATIVISTIC ELECTRON BEAM DIODE*

J.E. Coleman[§], D.C. Moir, C.A. Ekdahl, J.B. Johnson, B.T. McCuistian, and M.T. Crawford
Los Alamos National Laboratory, Los Alamos, NM, United States

Abstract

Explosive emission cathode studies are currently being conducted on a high power relativistic electron beam diode. A black velvet cathode is driven with a 75 Ohm graded transmission line, which provides a 3.8 MV, 80 ns (FWHM) pulse across a fixed A-K gap of 17.8 cm. Cathode sizes range from 1.9 – 7 cm with space-charge limited currents of 0.26 – 3 kA. The principal objective of these experiments is to quantify the current emission limits and the dynamics of the gap closure process. A qualitative comparison of experimental and calculated results are presented, which included the I-V relationship, impedance and perveance curves, plasma expansion velocity, and the time-resolved light emission on the surface of the cathode.

I. INTRODUCTION

Explosive emission cathodes have been used in the research and industrial communities for 40 years as a source of electrons [1,2]. These electrons are either accelerated and extracted to produce an intense relativistic electron beam, or they are terminated into a solid or perforated anode for high power microwave (HPM) production or flash X-ray radiography.

In accelerator applications, the electrons from cold cathodes are transported for long distances (tens of meters) and have been used for beam physics studies, high pressure gas propagation and the production of Bremsstrahlung radiation [3-8]. It is imperative to study the beam physics even in the accelerators used for radiography in order to optimize the radiographic spot size.

HPM production has been under investigation since the 1970s and cold cathodes are used in many of these facilities around the world. Cs-I doped carbon velvet has been explored by refs. [2,9] to mitigate gap closure, in relatively small diodes (~8 mm) with voltages >100 kV and currents >2 kA. Gap closure measurements have been performed on the KALI 5000, 3 cm diode with voltages up to 430 kV and currents of 17 kA [10]. Numerous velvet and graphite cathodes were studied with a solid SS anode; initial gap closure velocities as high as 40 cm/μs were measured then slowing to 10 cm/ μs. Explosive emission cold cathodes are also employed in virtual cathode oscillators for HPM production [11].

The RITS-6 machine, another radiographic facility, has also examined explosive emission with different diode geometries. A paraxial diode with a 4 cm A-K gap, 7.5 MV, 40 kA, 70 ns pulse was studied in addition to the self-magnetically pinched, hollow cathode diode, which produces 200 kA peak, ~60 kA across the diode [12]. LSP particle-in-cell simulations of the 1.2 cm diameter hollow cathode, 1.25 cm A-K gap have been performed in detail, indicating a cathode plasma density ~10^{17} cm^{-3} that migrates into the gap at ~50 cm/μs and an anode plasma of lower density ~10^{12} cm^{-3} that expands axially and radially in the opposite direction at relatively the same speed [13].

The first axis of the Dual-Axis Radiography for Hydrodynamic Testing (DARHT) facility is exploring the process of gap closure through the explosively emitting cold cathodes in motivation for the use of this cathode technology for longer pulsed and multi-pulsed operations [4]. In addition there is a motivation to continue to develop improved high brightness (B = J/ε) cold cathodes. We describe the emission as explosive because a strong electric field, >10 kV/cm, liberates electrons from the surface of the cathode, which desorb and ionize monolayers of gas deposited on the velvet surface. The primary electrons and ionized gas layers contribute to an avalanche of electrons, which is accelerated across the 17.8 cm gap, similar to a vacuum surface flashover. Secondary ions may impact the cathode and desorb more layers of gas creating an ionized cloud migrating off the surface at an unknown rate.

DARHT Axis-1 is unique for these studies because it has a relatively large A-K gap and does not have a solid or perforated anode as refs [2,9,10,12,13], reducing the contribution of the anode plasma to the gap closure velocity. Initial estimates indicate the closure velocity for this relativistic diode is ~ 10 cm/μs. These measurements are highly dependent upon the rise time of the diode voltage and the beam current as well as the I-V relationship. Since the diode is space-charge dominated and relativistic the I-V relationship is not easily modeled by the 1-D Child-Langmuir [14,15] or the Jory-Trivelpiece approximation [16] but more of a hybrid model.

II. EXPERIMENTAL SETUP

The experimental configuration used to study the gap closure dynamics on DARHT Axis-1 is shown in Fig. 1. A 75-Ω graded transmission line (or blumlein) provides the nominal 3.8-4 MV, 80 ns (FWHM) pulse (Fig. 2) to explosively drive the black velvet cathode. The voltage in the diode is monitored by a flush mounted coaxial E-dot

* This work was supported by the National Nuclear Security Administration of the U.S. Department of Energy under
§ email: jecoleman@lanl.gov

Report Documentation Page

Form Approved
OMB No. 0704-0188

1. REPORT DATE	2. REPORT TYPE	3. DATES COVERED
JUN 2013	**N/A**	**-**

4. TITLE AND SUBTITLE	5a. CONTRACT NUMBER
Explosive Emission And Gap Closure From A Relativistic Electron Beam Diode	5b. GRANT NUMBER
	5c. PROGRAM ELEMENT NUMBER
6. AUTHOR(S)	5d. PROJECT NUMBER
	5e. TASK NUMBER
	5f. WORK UNIT NUMBER
7. PERFORMING ORGANIZATION NAME(S) AND ADDRESS(ES) **Los Alamos National Laboratory, Los Alamos, NM, United States**	8. PERFORMING ORGANIZATION REPORT NUMBER
9. SPONSORING/MONITORING AGENCY NAME(S) AND ADDRESS(ES)	10. SPONSOR/MONITOR'S ACRONYM(S)
	11. SPONSOR/MONITOR'S REPORT NUMBER(S)

12. DISTRIBUTION/AVAILABILITY STATEMENT
Approved for public release, distribution unlimited

13. SUPPLEMENTARY NOTES
See also ADM002371. 2013 IEEE Pulsed Power Conference, Digest of Technical Papers 1976-2013, and Abstracts of the 2013 IEEE International Conference on Plasma Science. IEEE International Pulsed Power Conference (19th). Held in San Francisco, CA on 16-21 June 2013., The original document contains color images.

14. ABSTRACT
Explosive emission cathode studies are currently being conducted on a high power relativistic electron beam diode. A black velvet cathode is driven with a 75 Ohm graded transmission line, which provides a 3.8 MV, 80 ns (FWHM) pulse across a fixed A-K gap of 17.8 cm. Cathode sizes range from 1.9 7 cm with space-charge limited currents of 0.26 3 kA. The principal objective of these experiments is to quantify the current emission limits and the dynamics of the gap closure process. A qualitative comparison of experimental and calculated results are presented, which included the I-V relationship, impedance and perveance curves, plasma expansion velocity, and the time-resolved light emission on the surface of the cathode.

15. SUBJECT TERMS

16. SECURITY CLASSIFICATION OF:			17. LIMITATION OF ABSTRACT	18. NUMBER OF PAGES	19a. NAME OF RESPONSIBLE PERSON
a. REPORT	b. ABSTRACT	c. THIS PAGE			
unclassified	**unclassified**	**unclassified**	**SAR**	**6**	

aligned axially with the edge of the cathode shroud. The E-dot is mounted on the surface of the vacuum tank, ~1 m radially from the centerline of the diode. The E-dot picks up the capacitive charge voltage as voltage rises and falls on the cathode shroud. The integrated voltage waveform, zoomed into the peak, is shown in Fig. 2. There are four E-dots oriented azimuthally every 90° around the diode vacuum dome.

The extracted beam current is measured several places downstream, the first is Beam Position Monitor 1 (BPM 1) located just downstream of the diode at 24.5 cm and the next location is BPM 2 located at z = 82.4 cm. The BPMs consist of 8 B-dots, or inductive monitors, oriented azimuthally every 45°. There are 4 position B-dots, 1 top and bottom for ±y measurements and 1 left and right for ±x measurements. There are 4 more oriented at 45° relative to position B-dots that are used for current averaging over the cross section and as additional position measurements. The B-dots are simply a Type-N coaxial feedthrough with the center conductor soldered to an aluminum tab machined out of the inner cross section of the flange they are all housed in. The B-dots pick up the inductive image current as the beam head and tail pass by the B-dot. The amplitude of the signal is dependent on the proximity of the beam relative to the B-dot. A perfectly centered beam will have equal signals on each B-dot in a BPM housing, assuming each BPM has the same impedance. The integrated inductive image current measured at BPM 2, zoomed into the peak, is shown in Fig. 2.

In addition to the E-dots and BPMs, 2 image intensified, fast-gated, CCD cameras are mounted external to the cathode vacuum vessel [17]. The camera shown in the bottom of Fig. 1 is mounted parallel to the propagation axis of the beam and is used to view the light off the cathode surface and across the A-K gap. The camera shown in the top of Fig. 1 is mounted at a 30° angle to the propagation axis of the beam and is used to only view the light on the cathode face. The motivation behind these two configurations is to: first quantify the light intensity on the cathode face as a function of time and then if possible determine the light intensity as a function of the axial location and time away from the cathode face. If the light is substantial enough then time resolved gated images will provide an axial velocity profile of the plasma migration off the surface of the cathode. It is worth noting that the measured light intensity ~ n_e. $n_e < 10^{17}$ m^{-3} in the Axis-1 diode based on the electron beam current density, although it may be higher on the surface of the cathode and $n_o \sim 10^{18}$-10^{19} m^{-3}, assuming a 1-10% ionization fraction.

III. DIODE PERFORMANCE

The Axis-1 diode is routinely characterized when the cathode is conditioned from diode voltages of 2.2 – 4 MV. Since the diode is space-charge dominated, with dimensionless perveances of 5 x 10^{-5}-10^{-3} (depending on the cathode size used), and relativistic the I-V relationship is not easily modeled by the 1-D Child-Langmuir [14,15] or the Jory-Trivelpiece approximation [16]. So a hybrid model has been developed utilizing the 1-D Child-Langmuir, relativistic solutions, experimental measurements, and particle models using the TRAK code [18-20]. The standard 1-D Child-Langmuir Law has the expression:

$$J = \frac{4\varepsilon_o}{9}\sqrt{\frac{2q}{m_e}}\frac{V^{3/2}}{z^2}, \qquad (1)$$

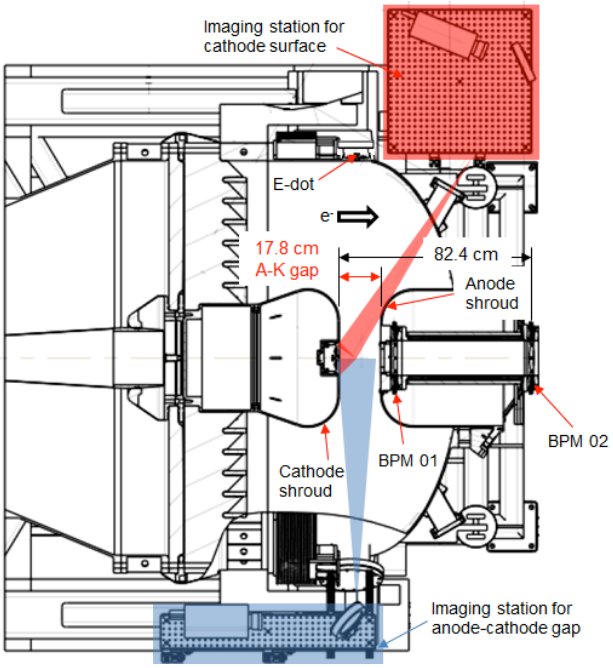

Figure 1. View of the DARHT Axis-1 diode with electrical and optical diagnostics used to diagnose the cathode plasma and electron beam. The imaging station for the cathode face is shaded in red and the imaging station for the A-K gap is shaded in blue.

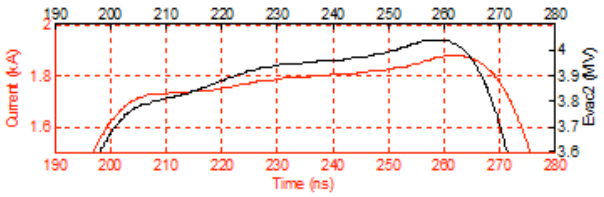

Figure 2. Blumlein voltage (black) used for explosive emission and extraction of the electron beam current (red) measured 82 cm downstream of the cathode face for the nominal 5 cm cathode.

where J is the current density, ε_o is the permittivity of free space, V is the applied diode voltage, and z is the diode A-K gap. The gun perveance, K_{gun} is defined as:

$$K_{gun} = \frac{4\varepsilon_o}{9}\sqrt{\frac{2q}{m_e}}, \qquad (2)$$

The hybrid model expresses the relationship between the beam current and voltage by including the gun perveance, which for this diode is 2.33 x 10^{-6} $A/V^{1.5}m^2$.

$$I = K_{gun} V^{*}, \qquad (3)$$

The power is expressed as * because as the beam becomes more and more relativistic I ~ V, for our model it is between 1.3 and 1.4. The accuracy of the model is shown below in Fig. 3. The extracted particle current calculated in TRAK for the nominal 5 cm cathode is displayed as a function of diode voltage. We extract a fit using Eq. 3 and compare it to the measured experimental values for 10 shots at relatively the same voltage. The experimentally measured current varies <1% over 10 shots for each voltage setting. TRAK calculates a current about 2-3% higher than experimentally measured.

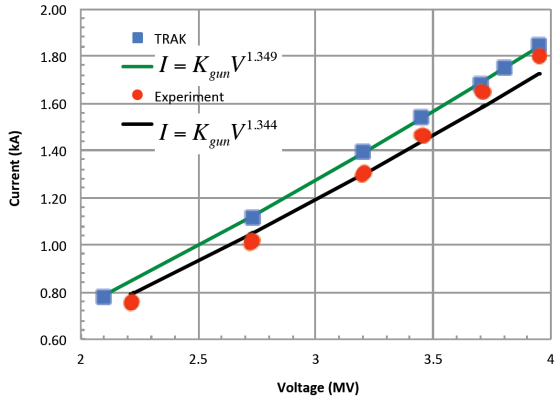

Figure 3. Current and voltage relation calculated in TRAK (blue squares) and the numerical fit calculated from Eq. 3 (green) compared with the experimentally measured values for 10 shots at each voltage (red circles) and the power fit for the experimental data set (black).

Referring to Fig. 2 we can see that we have a slight voltage and current ramp over the 60 ns window from 200-260 ns. The energy spread from head to tail is about ±2% from the center of the pulse.

Examining our nominal operating case, with a 5 cm cathode shown in Fig. 2, we calculate the time resolved power scaling for the experimental data from 200-260 ns (Fig. 4).

$$*(t) = \frac{\ln\left(\frac{I(t)}{K_{gun}}\right)}{\ln\left(V(t)\right)}, \qquad (4)$$

The time dependent power scaling is plotted below in Fig. 4(a); it oscillates between 1.3465 and 1.348. The time averaged power in Fig. 4(a) is <*> = 1.3473. In Fig. 4(b) we plot the I-V relationship over the pulse and the current tracks the voltage relatively linearly. We calculate the time averaged fit of the current using <*> = 1.3473 shown in green and it fits the data rather well.

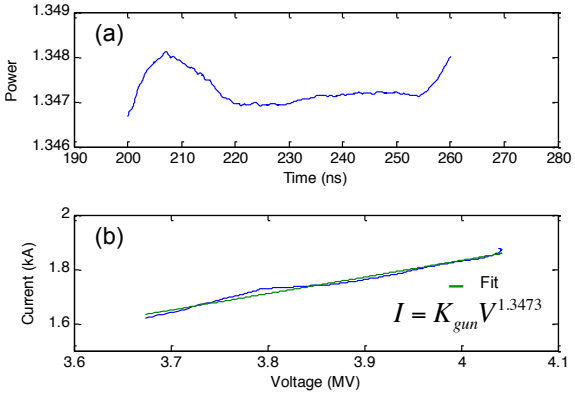

Figure 4. (a) The power relationship calculated from Eq. 4; (b) current and voltage relation over the 200-260 ns window (blue) and the time averaged fit (green), each for a single shot.

A diode voltage scan from 2.2-4 MV (Fig. 5) shows the average current and voltage mid-pulse (235-240 ns) for 10 shots at each level. In addition the time averaged power relation over the 235-240 ns window is shown. A calculated current fit is also shown where an average value of 1.344 is calculated for all voltage values over the 60 shots.

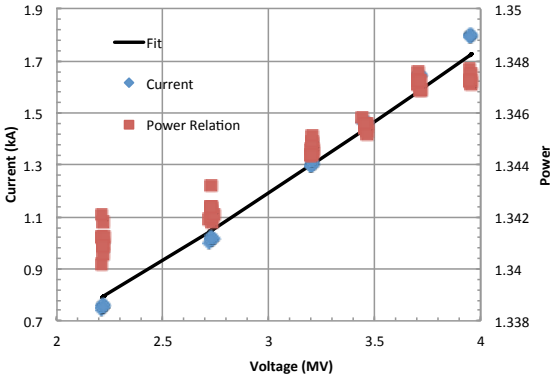

Figure 5. The average current vs. voltage from 235-240 ns is plotted (blue diamonds, left axis) and the time averaged power relation for each setting (red squares, right axis). Each setting has 10 shots, displaying the variation. The calculated current fit is shown (solid black, left axis).

Up to this point we have only considered the I-V relationship in one dimension for the nominal 5 cm cathode. On the Axis-1 diode we have also studied 3 additional cathode sizes which provide detailed information about the current density in 2-dimensions. We plan to investigate these details further and publish them at a later time.

IV. GAP CLOSURE MEASUREMENTS

In order to calculate the gap closure velocity it is necessary understand the I-V relationship developed in the previous section. Keep in mind these results are preliminary and highly dependent on the I-V relationship, in addition to the rise time of the diode voltage and extracted beam current as indicated below. Assuming a

space-charge dominated, relativistic diode the time dependent gap distance, $z(t)$, can be calculated as:

$$z(t) = \sqrt{\frac{K_{gun}\pi r^2 V(t)^*}{I(t)}}, \quad (5)$$

where r is the radius of the cathode. Simply taking the time derivative of $z(t)$, we can calculate the gap closure velocity:

$$v(t) = \frac{dz(t)}{dt}. \quad (6)$$

Prior to discussing the trends of the time dependent gap distance and closure velocity it is worth examining the rise time of the voltage and current waveforms in the diode (Fig. 6). The rise time of the voltage pulse monitored by the E-dot is 22 ns and the rise time of the current pulse monitored by BPM 2 is about 8 ns faster. We expect the beam current to begin to rise once the electric field > 30 kV/cm, which corresponds to V ~ 1.5 MV according to TRAK simulations. The cause of the differ rise times is not fully understood at this point, but may be explained by two effects. First the particle avalanche from the explosive emission may lead to runaway relativistic electrons, which accumulate faster than the voltage rises on the blumlein. Second, the intrinsic impedance of the BPM and E-dot are most certainly different. The BPM is a short at low frequency and the E-dot is a capacitor. Characterizing the impedance at GHz frequencies should determine the time response of each diagnostic.

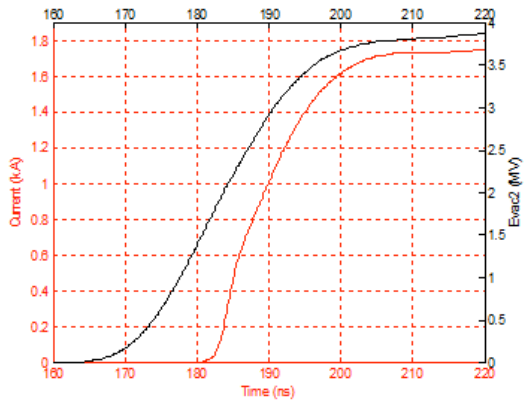

Figure 6. Current (red) and voltage (black) rise time for the nominal 5 cm cathode and 3.8 MV diode voltage.

The faster rise time of the current vs. the voltage helps explain the impedance collapse, perveance increase, and diode collapse we see below. First we examine the impedance, $Z(t)$, of the diode:

$$Z(t) = \frac{V(t)}{I(t)}. \quad (7)$$

With our nominal case of a 5 cm cathode and a 3.8 MV diode voltage, we extract an electron current of ~1.7 kA and expect an impedance of 2.2 kΩ. That is exactly what we measure near the middle of the pulse (210-260 ns) in Fig. 7. Since the impedance collapses through the rise of the current and voltage and remains relatively stagnant mid-pulse we expect the gun perveance

$$K_{gun}(t) = \frac{I(t)}{V(t)^*}, \quad (8)$$

to increase through the rise of the current and voltage and also remain constant mid-pulse (Fig. 7). The gun perveance is labeled as μPerveance in Fig. 7 because the arbitrary units are of the order 10^{-6}.

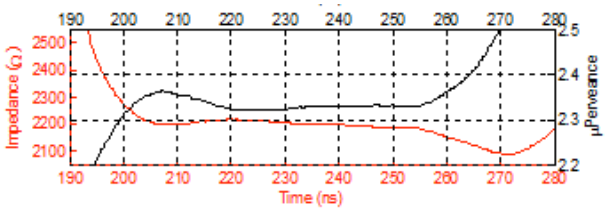

Figure 7. Impedance (red) and μPerveance (black) for the nominal 5 cm cathode and 3.8 MV diode voltage. The perveance is labeled as μPerveance because the arbitrary units are of the order 10^{-6}.

Since the impedance in the diode is collapsing as a function of time it is logical that the A-K gap distance should close at a rate ~$K_{gun}^{-1/2}$. Examining Fig. 8, generated from Eqs. 5 & 6, on the same relative time scale as Figs. 2 & 7 we can see that the gap is reduced from the physical 17.8 cm to < 5 cm through the rise time of the pulse (t < 190 ns). This initial closure rate is quite fast compared to closure velocities measured in the literature, although once the voltage and current pulses (Fig. 6) have reached the later portion of their rise time (t > 190 ns) the velocities are more reasonable ~10 cm/μs. Once the voltage and current reach the end of their rise time (t ~ 205 ns) the gap distance becomes stagnant at 4.5 cm and does not begin to close further until the end of the pulse (t > 250 ns). Keep in mind these results are preliminary and highly dependent on the I-V relationship, in addition to the rise time of the diode voltage and extracted beam current. Also, although the gap may have collapsed to this level, there is no longer a single emission surface from which current can be extracted, so the beam current may not increase proportional to $1/z^2$.

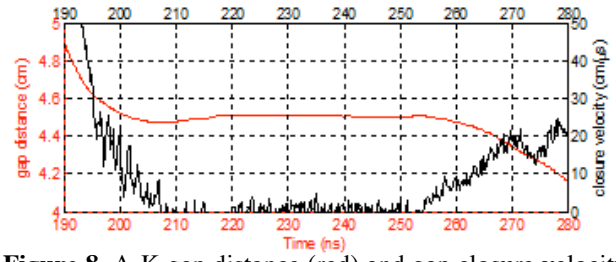

Figure 8. A-K gap distance (red) and gap closure velocity (black) for the nominal 5 cm cathode and 3.8 MV diode voltage.

A summary of the gap closure measurements made with the 5 cm cathode was evaluated as a function of diode voltage (Fig. 5). The diode voltage was varied from 2.2-4 MV and using the I-V power relation derived in Eq. 4 and plotted in Fig. 4(a), we measured and calculated the A-K gap distance and the gap closure velocity. The average values near the end of the voltage and current rise times (200-205 ns) are plotted in Fig. 9 for 10 shots at each level. There is a small variation, >1%, in the calculated gap distance at all diode voltages. However, there is substantial shot variation in the calculated closure velocity, at low voltage (2.2 MV) it is 9.89 ± 5.83 cm/μs, nearly 60%. At 3.95 MV the variation in the closure velocity is reduced, to ~18%, with a rate of 8.5 ± 1.52 cm/μs.

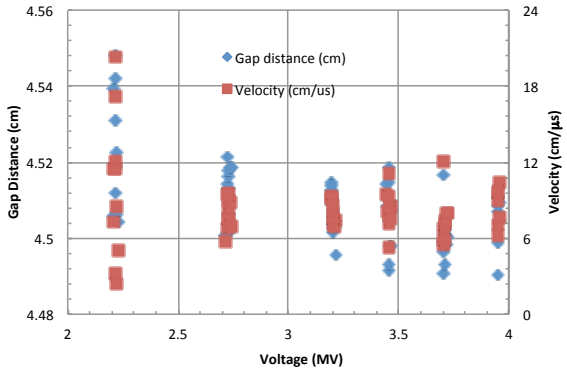

Figure 9. A-K gap distance (blue diamonds, left axis) and gap closure velocity (red squares, right axis) averaged over 200-205 ns for 10 shots at each voltage with the nominal 5 cm cathode as a function of diode voltage.

These measurements are still preliminary and rely on the performance of the E-dot and BPM diagnostics. Capacitive and inductive loading on the diagnostics can effect the rise time and require further investigation. As mentioned above, we plan to field optical diagnostics to help better explain these phenomena, in addition we are beginning PIC simulations of the explosive emission process. Preliminary results from the optical measurements are discussed below.

V. CATHODE IMAGING

We have begun to field optical diagnostics for imaging the light on the cathode surface and across the A-K gap as stated in Section II and shown in Fig. 1. We will only report the preliminary images of the cathode face (red shaded region in Fig. 1). Fig. 10 below shows two images of the cathode face, recall that these are images reflected off a mirror with the camera axis at a 30° angle relative to the beam propagation axis, explaining the elliptical profile on the charge–coupled device (CCD). This is done to help minimize any direct X-ray flux onto the micro-channel plate and CCD, additional high-Z shielding material is also required for these measurements to minimize any additional counts on the CCD that are not visible photons. The image on the left (Fig. 10(a)) is a 500 μs open shutter of the 7-cm cathode face and surrounding anodized aluminum shroud; this was taken without pulsing the diode. The image on the right (Fig. 10(b)) is a 20 ns gate of the explosive emission on the cathode face in the middle of the extraction pulse (t = 215 ns). Despite the shielding efforts, there is still scattered speckles on the image in Fig. 10(b) that we believe are prompt scattered soft X-rays and plan to characterize them in the future. The triggering of the camera gate is synchronized with the onset of the blumlein voltage in the diode and is monitored in parallel with the E-dot and BPM diagnostics to verify the gate time is accurate. We have acquired multiple gated images with extended delays and have determined that the cathode plasma continues to emit light ~9 μs after the initial rise of the voltage on the blumlein. It is important to point out that the blumlein is not perfectly matched. After the initial extraction, the voltage reverses at t = 300 ns and continues to ring underdamped with a positive voltage of 1.5 MV and then another negative voltage of ~1 MV and continues to dampen out to negligible voltage at ~ 3.5 μs (Fig. 11(a)).

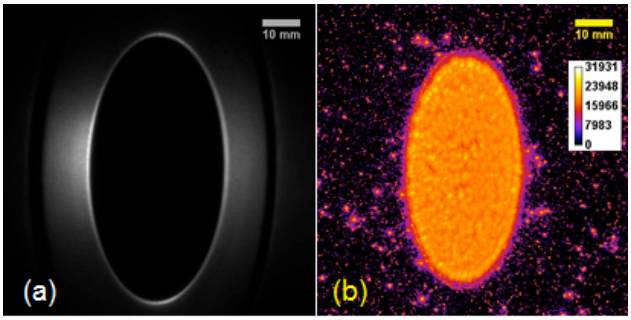

Figure 10. (a) Open shutter calibration image of a 7-cm diameter cathode installed in the Axis-1 diode; and (b) 20 ns gate of the explosive emission on the cathode face in the middle of the extraction pulse (t = 215 ns) (log scale, false color).

We have also examined the temporal light intensity with respect to the voltage (Fig. 11(b)) used to extract current from the diode (Fig. 11(c)). It is interesting to point out that the integrated light intensity for each 20 ns gated image maps well to the current profile. Indicating when the voltage is negative again at t ~ 400 ns, electrons are extracted from the existing illuminated plasma at this time.

The light we see during the main extraction pulse is fairly uniform across the surface of the cathode with random intense spots. This light is most likely excitation of the desorbed and ionized monolayers of gas on the surface of the cathode. Further diagnosis of this process will be performed with more quantitative imaging, spectral line intensity, and broadening measurements particularly across the A-K gap. These include temporally and spatially resolved spectroscopy of the light emission [12,21]. This will not only provide additional confirmation of the plasma migration off the surface of the cathode, but the line intensities can be used for both ion Doppler broadening measurements (measure T_i) and gas impurity line measurements (infer T_e) [22]. Each of these measurements will provide further clarification of the gas desorption, ionization process, and gap closure velocity of the explosive emission plasma.

VI. CONCLUSIONS

We have effectively measured the time dependent extraction voltage, beam current, and gun impedance.

Initial results indicate our gap closure velocity <10 cm/μs. These measurements are still in their infancy and are highly dependent on the I-V relationship, in addition to the rise time of the diode voltage and extracted beam current. However, they do agree fairly well with measurements in the literature for different diode geometries.

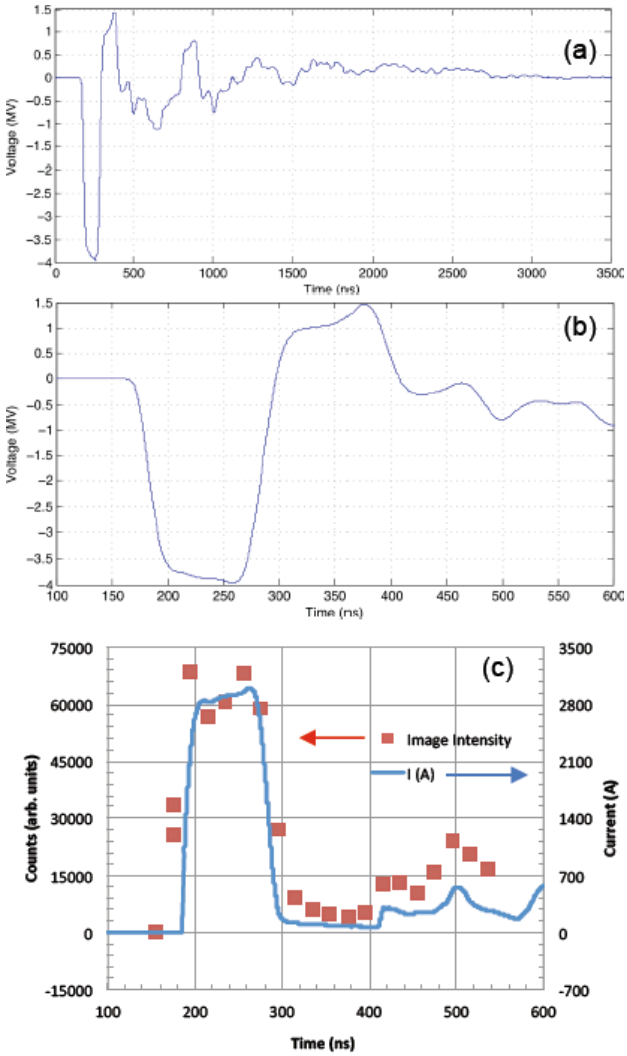

Figure 11. (a) Full voltage pulse applied to the cathode (0-3.5 μs); and (b) narrower time window of voltage pulse (100-600 ns); (c) integrated light intensity for each 20 ns gated image (red squares, left axis) compared with the current extracted from the diode (blue, right axis).

In addition we have begun to image the explosive emission on the cathode face. The light appears to be fairly uniform and lasts 9 μs after the initial rise of the voltage in the diode. In addition the light intensity on the cathode surface maps pretty well with the extracted electron current profile. Further characterization of the explosive emission will be diagnosed with more quantitative imaging and spectral line intensity and broadening measurements.

VII. REFERENCES

[1] R.B. Miller, "Mechanism of explosive emission for dielectric fiber (velvet) cathodes," J. Appl. Phys., vol. 84, (no. 7), pp. 3880- 3889, (1998).

[2] D. Shiffler, "Review of Cold Cathode Research at the Air Force Research Laboratory," IEEE Trans. Plasma Sci., vol. 36, no. 3, pp. 718 (2008).

[3] C.H. Jackson, "The Advanced Test Accelerator (ATA) Injector," IEEE Transactions on Nuclear Science, Vol. NS-30, No. 4, 1983.

[4] G. Westenskow, "Double pulse experiment with a velvet cathode on the ATA injector," in Proceedings of the Particle Accelerator Conference, Dallas, TX, 1995 (IEEE, Dallas, TX 1995), pp. 1027.

[5] E. Merle, "Transport optimization and characterization of the 2 kA AIRIX electron beam, Proc of XXth LINAC conf., pp. 494 (2000).

[6] C. Ekdahl, "Modern Electron Accelerators for Radiography," IEEE Trans. Plasma Sci., vol. 30, no. 1, pp. 254 (2002).

[7] T.L. Houck, "Recent Flash X-ray Injector Modeling," UCRL-TR-208574 (2004).

[8] H. Dzitko, "Operational efficiency of the AIRIX accelerator since its commissioning," in Proceedings of IPAC2012, New Orleans, LA, USA, pp. 4017 (2012).

[9] C.F. Lynn "Light Emission from CsI-Coated Carbon Velvet Cathodes under Varied Conditions," IEEE Trans. Plasma Sci., vol. 40, no. 12, pp. 3449 (2012).

[10] A. Roy, "Plasma expansion and fast gap closure in a high power electron beam diode," Phys. Plasmas, vol. 16, pp. 053103 (2009).

[11] Y.-J. Chen "Compact, repetitive Marx generator and HPM generation with the VIRCATOR," MS thesis, Texas Tech University, 2005.

[12] K. Hahn, "Overview of Self-Magnetically Pinched-Diode Investigations on RITS-6," IEEE Trans. Plasma Sci., vol. 38, 2652 (2010).

[13] D.R. Welch, "Hybrid simulation of electrode plasmas in high-power diodes," Phys. Plasmas, vol. 16, pp. 123102 (2009).

[14] C. D. Child, "Discharge from hot CaO," *Phys. Rev.*, vol. 32, no. 5, pp. 492–511, 1911.

[15] I. Langmuir, "The effect of space charge and residual gases on thermionic currents in high vacuum," *Phys. Rev.*, vol. 2, no. 6, pp. 450–486, 1913.

[16] H. R. Jory and A. W. Trivelpiece, "Exact relativistic solution for the one-dimensional diode," J. Appl. Phys., vol. 49, (no. 10), pp. 3924-3926 (1969).

[17]http://www.princetoninstruments.com/products/imcam/pimax/

[18] Stanley Humphries Jr., "TRAK – Charged particle tracking in electric and magnetic fields," in Computational Accelerator Physics, R. Ryne Ed., New York: American Institute of Physics, 1994, pp. 597-601.

[19] Stanley Humphries Jr., *Field solutions on computers,* (CRC Press Boca Raton, FL 1997) and www.fieldp.com.

[20] C.A. Ekdahl, "Axis-I Diode Simulations I: Standard 2-inch cathode," LA-UR-11-00206 (2011).

[21] M.D. Johnston "Absolute calibration method for nanosecond-resolved, time-streaked, fiber optic light collection, spectroscopy systems," Rev. Sci. Instrum., vol. 83, pp. 083108 (2012).

[22] P.G. Carolan, "The behaviour of impurities out of coronal equilibrium," Plasma Phys., vol. 25, no. 10, pp. 1065 (1983).